

## PRECISE MODELING OF ANTENNA TOWERS

*This paper is dedicated to Professor Jovan Surutka  
on the occasion of his 80<sup>th</sup> birthday*

**Miodrag S. Tasić, Branko M. Kolundžija  
and Antonije R. Đorđević**

**Abstract:** Modern numerical methods can be used for very precise modeling of antenna towers. However, creation of precise models can be very tedious and the corresponding analysis can be very time consuming. The paper investigates under which conditions the complex antenna towers can be equivalented by single-wires.

**Key words:** Antenna tower, thin-wire analysis, numerical modeling.

### 1. Introduction

VLF, LF and MF ranges extends over a very large range of wavelengths, from 100 km to 100 m. This means that realizable structures are small with respect to the wavelength at VLF, while at MF the electrical height of antennas can be one-half wavelength or little bit more. In order to maximize the radiation efficiency these antennas should be made as much physically large as possible. Typical antenna heights employed for broadcasting in these frequency ranges are from 50 m to 300 m [1].

The antennas are usually realized as variants of monopole antennas that can be top-loaded and as simple arrays of such antennas. The monopole antennas, which are relatively fat, can be realized as self-supporting towers. The monopole antennas, which are relatively thin (e.g. anti-fading antennas), are made in the form of cages or cylindrical masts, which must be

---

Manuscript received August 22, 2001. A version of this paper was presented at the fifth IEEE Conference on Telecommunication in Modern Satellite, Cables and Broadcasting services, TELSIS 2001, September 19-21, 2001, Niš, Serbia.

The authors are with University of Belgrade, Department of Electrical Engineering, Bul. Kralja Aleksandra 73, 11120 Belgrade, Serbia (e-mail: kol@kiklop.etf.bg.ac.yu).

supported by guy ropes or self-supporting towers. In what follows all such monopole antennas will be termed as antenna towers. One typical antenna that contains different types of antenna towers is the cage T-type radiator suspended between two grounded self-supporting towers, as shown in Fig. 1 [2].

Not only construction of antenna towers is very expensive, but also construction of scaled models for laboratory purposes. Hence, it is very important to have analytical and/or numerical tools that enable fast and accurate evaluation of antenna characteristics. At the beginning (after the work of Pocklington in 1897 [3]) simple monopole antennas were treated as single wires and sinusoidal approximation along these wires was assumed. For example, using the method of induced electromotive force Labus determined input impedance of simple monopole antenna in 1933 [4]. However, such approximation is justified only for very thin wires. The influence of wire thickness was first taken into account by Siegel and Labus in 1934, which was derived from theory of lossy transmission lines [5]. The influence of wire thickness was taken more precisely into account by Hallen in 1938, who iteratively solved the integro-differential equation, later called by his name [6]. R. W. P. King and his associates analyzed many wire antennas using improved Hallen's method, which culminated in his classical monograph in 1956 [7]. However, the method applied by King was still very limited: a) basically, it is analytical method that required high knowledge to be applied to new structures, and b) it can not handle multiple wire structures.

New era in analysis of wire structures has begun with method of moments [8], which is introduced in numerical electromagnetics by Harrington in 1968. The MoM enabled numerical solution of integral equations for currents along various thin-wire structures, including multiple wire junctions [9], [10]. ("Thin-wire" means that current over wire surface has only axial component dependent only on axial coordinate. This assumption is also called "thin-wire approximation".) Based on this theory a variety of commercial software packages appeared (e.g. AWAS in 1991 [11]), which enables analysis of arbitrary wire structure even to users not familiar with numerical modeling.

In some cases, "thin wire approximation" does not give accurate or even acceptable results (e.g. for fat wires, or for close wires, where proximity effect is pronounced, etc.) [12]. These cases wire structures need to be modeled partly or completely as solid metallic body (by plates). In that case both components of surface current should be represented as dependent on two independent surface coordinates. There are also many commercial software

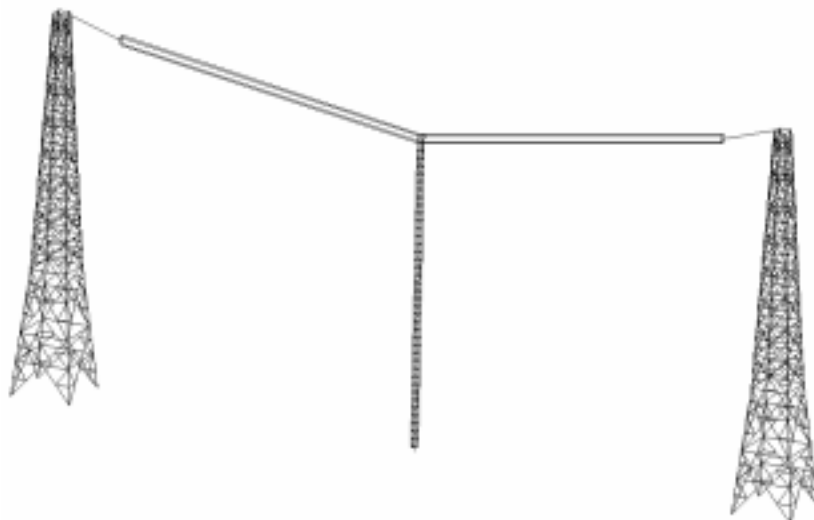


*Fig. 1. The cage T-type radiator suspended between two grounded self-supporting towers.*

packages that can handle solid metallic bodies (e.g. WIPL-D [13]).

Obviously, modern numerical software packages enable very precise modeling of composite wire and plate structures, including antenna towers. For example, the antenna shown in Fig. 1 can be modeled in detail, using 3376 wires. However, such analysis takes a lot of CPU time (e.g. 1 hour per frequency at Pentium 2 on 450 MHz). Experience from the past shows that very good results can be obtained if a complex tower structure is equivalented by single wire. In that case the antenna shown in Fig. 1 can be modeled by only 8 wires. Such analysis is finished in whole frequency range in less than 1 sec. Hence, such model is very suitable for an optimization.

The question is how precisely one should model antenna tower to obtain enough accurate results. To answer to this question let us first introduce techniques for precise modeling of composite metallic structures in Section 2. These techniques will be applied in Section 3 to different antenna towers, giving us information about optimal modeling. Finally, the optimal modeling will be applied to some complex examples in Section 4.

## **2. Precise Modeling of Composite Wire and Plate Structures**

Analysis of composite wire and plate structures is usually based on the MoM solution of Electric Field Integral Equations (EFIEs) [14,15]. The

EFIE is obtained starting from the boundary condition that tangential component of electric field is equal to zero over metallic surfaces and expressing this field in terms of known impressed field and field due to unknown induced currents. According to the MoM the unknown currents in the EFIE are expanded into finite series of known basis functions multiplied with unknown coefficients. The EFIE is multiplied with known test functions and integrated throughout the domains of the test functions, resulting in a system of linear equations. Using standard methods (Gaussian elimination, LU decomposition) the unknown coefficients are easily determined. Very precise modeling of composite structures can be achieved if basis and test functions are properly adopted. Very good choice for test functions is when they are equal to basis functions. This variant of MoM is known as the Galerkin method. Choice of test functions is performed into two steps: geometrical modeling and approximation of currents. Very flexible approximation of currents is achieved by using polynomial basis functions that automatically satisfies continuity of currents at wire and plate ends and junctions. In what follows particular attention will be paid to geometrical modeling of wires, plates, wire-to-plate junctions, plate modeling of wires and wire-grid modeling of plates, which is of the most interest from the view-point of precise modeling of antenna towers.

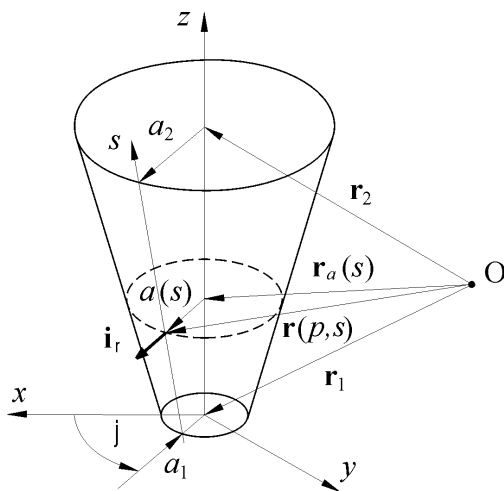


Fig. 2. Right truncated cone.

Very flexible geometrical modeling of wires can be performed by right truncated cones. A right truncated cone is determined by position vectors

and radii of its beginning and its end,  $\mathbf{r}_1$  and  $a_1$ , and  $\mathbf{r}_2$  and  $a_2$ , respectively, as shown in Fig. 3. The parametric equations of the cone axis and its local radius can be written in the form

$$\mathbf{r}_a(s) = \frac{1-s}{2}\mathbf{r}_1 + \frac{1+s}{2}\mathbf{r}_2, \quad -1 \leq s \leq 1, \quad (1a)$$

$$a(s) = \frac{1-s}{2}a_1 + \frac{1+s}{2}a_2, \quad -1 \leq s \leq 1, \quad (1b)$$

where  $s$  is local coordinate along a cone generatrix. In order to define parametric equation of the cone surface, let us adopt a local cylindrical coordinate system in such a manner that the  $z$ -coordinate axis coincides with the cone axis. In that case the parametric equation of the cone surface can be written as

$$\mathbf{r}(\phi, s) = \mathbf{r}_a(s) + a(s)\mathbf{i}_\rho(\phi), \quad -1 \leq s \leq 1, \quad -\pi \leq \phi \leq \pi, \quad (2)$$

where  $\phi$  is the circumferential angle, measured from the  $x$ - axis, and  $\mathbf{i}_\rho(\phi)$  is the radial unit vector, perpendicular to the cone axis.

As special cases, the truncated cone degenerates into a right cylinder ( $a_1 = a_2$ ), an ordinary cone ( $a_2 = 0$ ), a flat disc ( $a_2 = 0$ ,  $\mathbf{r}_1 = \mathbf{r}_2$ ), and a frill ( $\mathbf{r}_1 = \mathbf{r}_2$ ). The right truncated cone and its degenerate forms can be used for modeling of cylindrical wires with flat (frill-like) or conical changes of the wire radius, as well as of flat and conical wire ends and feeds.

Metallic surfaces are modeled by bilinear surfaces. A bilinear surface is, in general, a nonplanar quadrilateral, which is defined uniquely by its four arbitrarily spaced vertices, as shown in Fig. 3. Hence, it can be used for efficient modeling of both flat and curved surfaces. The parametric equation of element can be written in the form

$$\begin{aligned} \mathbf{r}(p, s) = & \mathbf{r}_{11} \frac{(1-p)(1-s)}{4} + \mathbf{r}_{12} \frac{(1-p)(1+s)}{4} \\ & + \mathbf{r}_{21} \frac{(1+p)(1-s)}{4} + \mathbf{r}_{22} \frac{(1+p)(1+s)}{4} \end{aligned} \quad (3)$$

$$-1 \leq p \leq 1, \quad -1 \leq s \leq 1$$

where  $\mathbf{r}_{11}$ ,  $\mathbf{r}_{12}$ ,  $\mathbf{r}_{21}$ , and  $\mathbf{r}_{22}$  are the position vectors of its vertices, and  $p$  and  $s$  are local coordinates. After elementary transformations this equation can be written as

$$\begin{aligned} \mathbf{r}(p, s) = & \mathbf{r}_c + \mathbf{r}_p p + \mathbf{r}_s s + \mathbf{r}_{ps} ps \\ & -1 \leq p \leq 1, \quad -1 \leq s \leq 1 \end{aligned} \quad (4)$$

where  $\mathbf{r}_c = (\mathbf{r}_{11} + \mathbf{r}_{12} + \mathbf{r}_{21} + \mathbf{r}_{22})/4$ ,  $\mathbf{r}_p = (-\mathbf{r}_{11} - \mathbf{r}_{12} + \mathbf{r}_{21} + \mathbf{r}_{22})/4$ ,  $\mathbf{r}_s = (-\mathbf{r}_{11} + \mathbf{r}_{12} - \mathbf{r}_{21} + \mathbf{r}_{22})/4$  and  $\mathbf{r}_{ps} = (\mathbf{r}_{11} - \mathbf{r}_{12} - \mathbf{r}_{21} + \mathbf{r}_{22})/4$ . Depending on the values of the vectors  $\mathbf{r}_p$ ,  $\mathbf{r}_s$ , and  $\mathbf{r}_{ps}$ , a bilinear surface takes different degenerate forms: flat quadrilateral ( $\mathbf{r}_p$ ,  $\mathbf{r}_s$ , and  $\mathbf{r}_{ps}$  are coplanar), rhomboid ( $\mathbf{r}_{ps} = 0$ ), rectangle ( $\mathbf{r}_{ps} = 0$  and  $\mathbf{r}_p \cdot \mathbf{r}_s = 0$ ), etc.

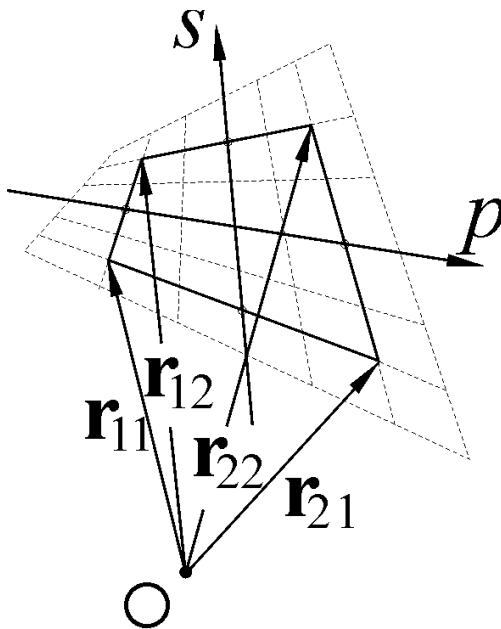


Fig 3. Bilinear surface.

Geometrical modeling of wire-to-plate junctions is performed using specific segmentation technique, as shown in Fig 4. Each plate at the junction is subdivided into two, three or four plates in such a manner that short edges of subplates surround the wire end. In addition, it is forced that total current flowing out from the junction domain (consisting of the short edges and the wire end) is zero [16].

If wires are fat, or mutually very close such that proximity effect is pronounced, precise modeling requires that wire be represented as plate structure. For example, cylindrical part of wire can be represented by four (six, eight) narrow strips, in which case the cross-section the of equivalent wire is square (hexagon, octagon). In that case the wire end is represented by one (two, four) plates. It is shown that very good results can be obtained even with small number of strips, if surface area of the cross-section of the

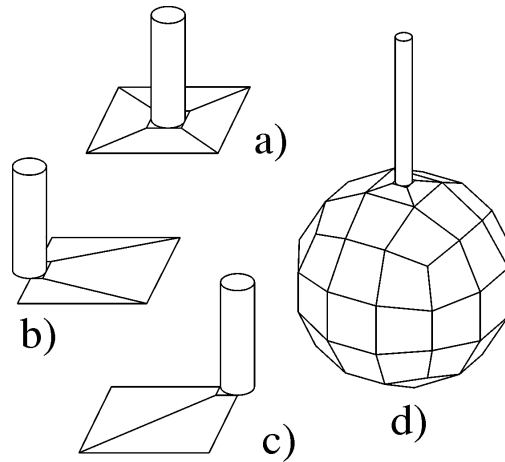


Fig 4. Wire-to-plate junctions.

equivalent wire is equal to the surface area of the circular cross-section of original wire.

In some cases it is convenient to represent plate structure by wire grids and vice versa, wire grid model by plates [17]. A plate is represented by wire grid in the following way. First step is to subdivide bilinear surface into  $N + 1$  strips along  $s$ -axis, where  $N$  is dividing factor, as illustrated for  $N = 4$  in Fig. 5(a). (In this case, for convenience, starting and ending  $p$  and  $s$ -coordinates are adopted to be 0 and 1.) Subdivision is performed by a set of  $N + 2$   $s$ -coordinate lines, whose  $p$ -coordinates are  $p_0 = 0$ ,  $p_i = (2i - 1)/2N$ ,  $i = 1, \dots, N$ ,  $p_{N+1} = 1$ . Note that widths of all inner strips are approximately equal, while widths of outer strips are approximately twice smaller. Next step is to replace each strip with the equivalent wire. For an inner strip the equivalent wire is placed in the middle of the strip, while for outer strip the equivalent wire is placed along the edge of bilinear surface, as shown in Fig. 5(b). The radius of the equivalent wire is determined as  $r = F*w/2$ , where  $w$  is strip width and  $F$  is fulfillment factor. In general case the strip width changes linearly along the strip. Hence, the equivalent wire is obtained in the form of a right truncated cone. (Such kind of wires is supported by software package WIPL-D.) It is obvious that thus obtained set of wires approximate  $s$ -current component of starting plate. In a similar way we obtain a set of wires that approximate the  $p$ -current component of starting plate, as shown in Fig. 5(c). Finally, we combine these two sets of wires into a wire grid, as shown in Fig. 5(d).

The same procedure is applied to all plates in starting solid surface model. In particular, let us consider junction of two plates, as shown in Fig. 6(a). In order that wire-grid models of these plates can be correctly connected, both plates need to be meshed with the same dividing factor  $N$ , as shown in Fig. 6(b). Besides that, note that after meshing of connected plates we obtain that  $N + 1$  wires of one wire grid, which are placed along the junction of the plates, coincide with  $N + 1$  wires of another wire grid. Obviously, each pair of coinciding wires should be merged into single wire. To maintain the fulfillment factor the radius of thus obtained wire should be equal to the sum of radii of original wires, as shown in Fig. 6(c).

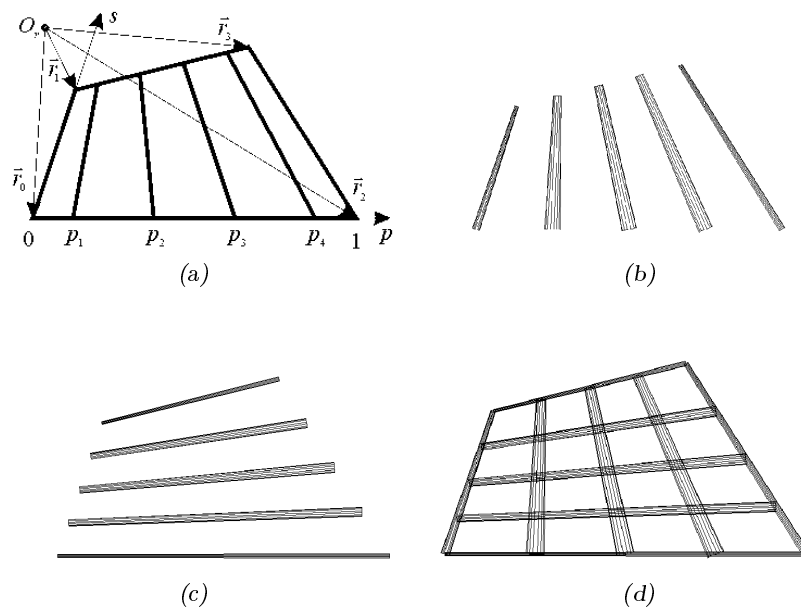


Fig. 5. Conversion of a bilinear surface into a wire grid.

Thus, very general algorithm for automatic wire-grid modeling is obtained. By numerical experiments it is found that in most cases best matching with solid surface model is achieved if fulfillment factor correspond to the “same surface area” rule ( $F = 0.32$ ). Besides that it is found that practically all cells in wire grid should be enough small, e.g. smaller than  $0.1\lambda \times 0.1\lambda$ . Obviously, it is optimal that all cells be of approximately the same size.

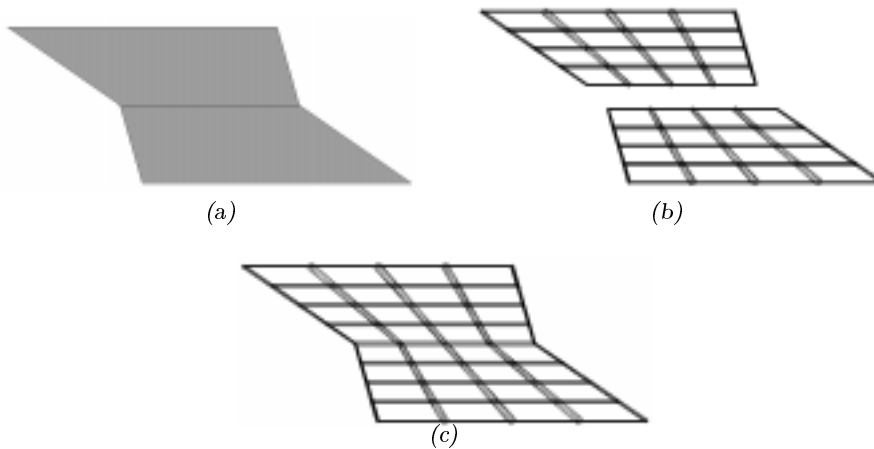


Fig. 6. Wire grid modeling of two connected plates.

### 3. Various Models of Antena Towers

Very precise model of antenna tower takes into account its mechanical construction, as shown in Figs. 7(a), (b), (c) and (d). Basically the construction consists of rectangular cells. The cell can be empty (model “empty” shown in Fig. 7(a), or it can contain: diagonal rod (model “diagonal” shown in Fig. 7(b), two rods (model “triangle” shown in Fig. 7(c), four rods (model “diamond” shown in Fig. 7(d), etc. All these models can be considered as wire-grid models of solid metallic tower (modeled by 9 plates), as shown in Fig. 7(e). Finally, solid tower can be equivalented by three wires of (conical wire at feed, long cylindrical wire and flat disk wire at the top of the tower), as shown in Fig. 7(f). This model will be termed as simplified wire model.

Let us compare results for input impedance if tower height is  $h = 110$  m and base width is  $a = 10$  m. Fig. 9 shows result for plate and simplified model. Very good agreement between results is observed, which means that equivalence between plate and simplified wire model is valid even for relatively thick towers. Figs. 10(a) and (b) shows results for the “empty” and the “triangle” model for different radii of wires compared with plate model. It is seen that by increasing the radii the result obtained by the “empty” model approaches to the results obtained by plate model. This is explained by the fact that “fulfillment factor” of the “empty” model approaches to its optimal value of  $F = 0.32$ . Results obtained by “triangle” model shows better convergence to the “plate” model then result obtained by the “empty”

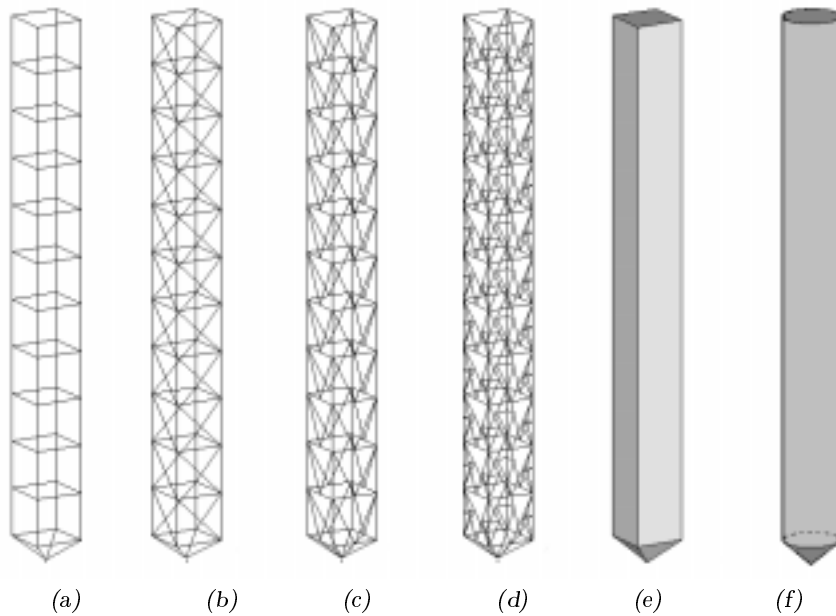


Fig. 7. Different cage models.

model. This is explained by the fact that for the same radius the fulfillment factor of “triangle” model is almost doubled when compared with that of the “empty” model. In addition the cells in the “triangle” model are three times smaller than cells in the “empty” model.

However, for thin cages the results are not much dependent of the fulfillment factor. For example, let us consider tower broadcast MF antenna supported by four guy ropes, as shown in Fig. 8. The tower height is  $h = 110$  m and base width is  $a = 2$  m. The ropes are connected to the tower at height of 79.2 m and grounded at distance 72.6 m from the tower. Diameter of ropes is 3 m. Fig. 8(a) shows simplified wire model, while Figs. 8b, c, and d shows “empty”, “diagonal” and “triangle” models of the tower respectively. Radius of wires in last three models used for the tower is 5 cm, which means that fulfillment factor is relatively low. Fig. 11 shows result for input admittance for all four models. It is concluded that for thin towers the results are not much dependent on fulfillment factor.

Having in mind above results and some other results not shown here, we can conclude: the simplified wire model can be used for precise analysis of thin towers and those thick towers, whose fulfillment factor is relatively large.

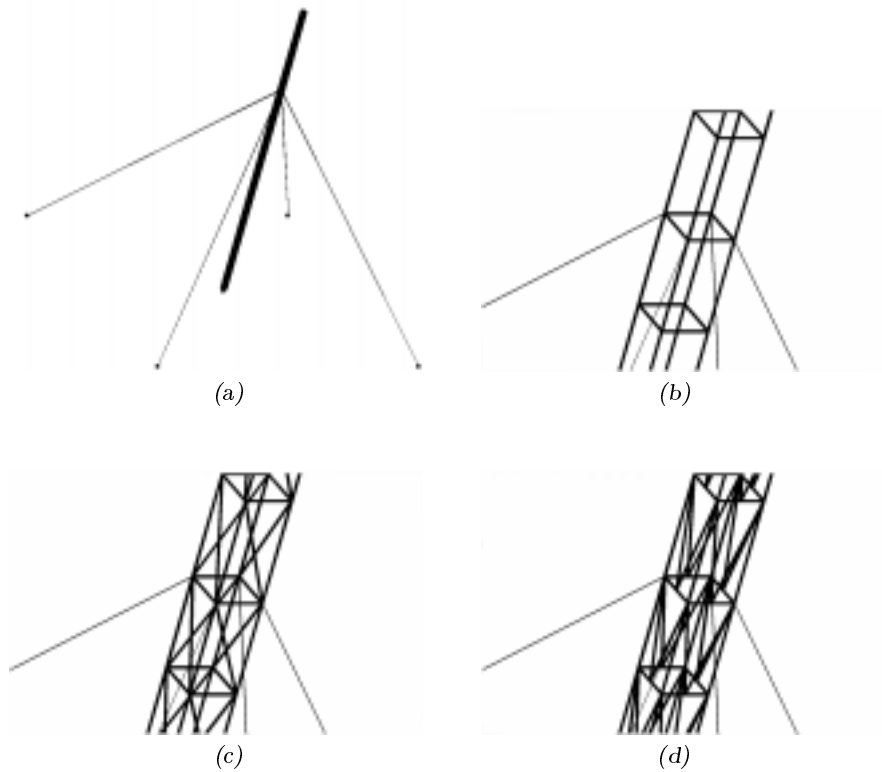


Fig. 8. Different models of tower broadcast MF antenna:  
 (a) simplified wire model, (b) model "empty",  
 (c) model "diagonal" and (d) model "triangle".

For precise analysis of thick towers, whose fulfillment factor is relatively small, their mechanical construction should be modeled in detail. Particular case, when even thin cage tower can not be equivalented by single wire is the case when an antenna mast is placed inside the cage, so that the cage has partial screening effect with respect to the tower.

#### 4. Numerical Examples

As a first example, let us consider the T-antenna shown in Fig. 1. It is obvious that the T-antenna itself belongs to the class of thin towers, while supporting towers belong to the class of thick towers. The simplified wire model is shown in Fig. 12. According to the conclusions at the end of previous section the simplified wire model is satisfactory for the T-antenna,

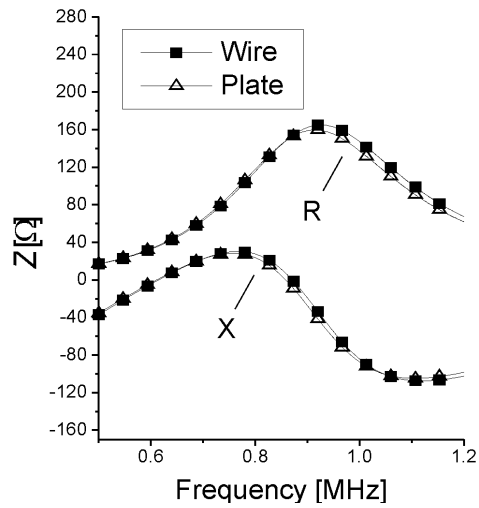


Fig. 9. Input impedance of simplified wire model and plate model of tower antenna shown in Fig. 7.

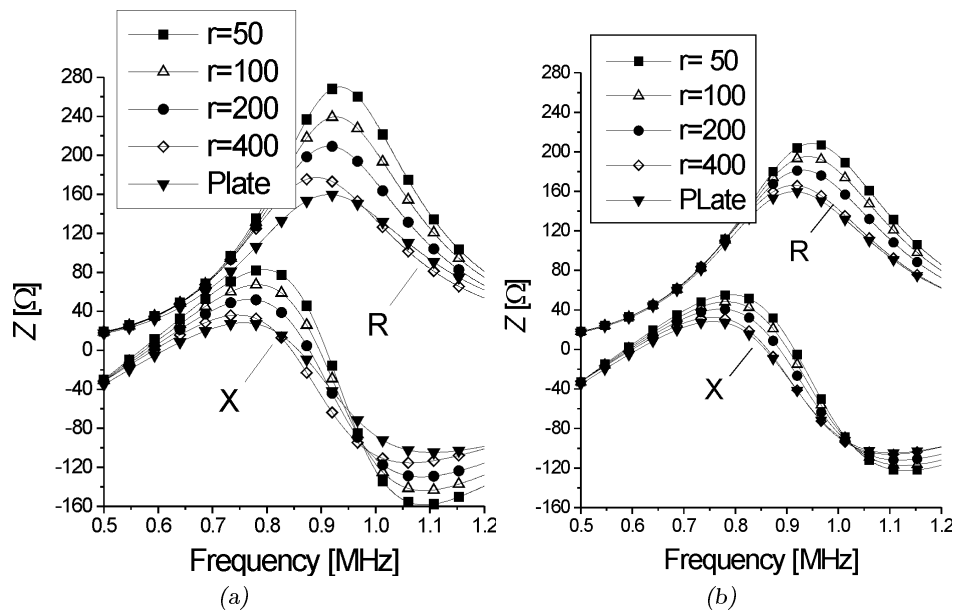


Fig. 10. Input impedance of “empty” model (a) and “triangle” model (b) compared with that of “plate” model of the tower (all shown in Fig. 7), for different wire radii.

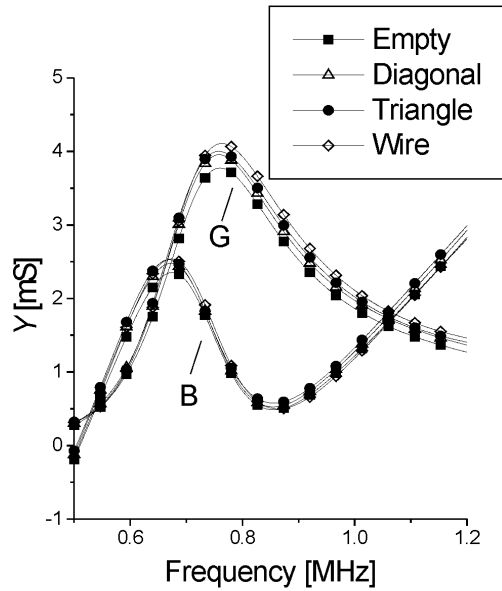


Fig. 11. Input admittance of tower broadcast MF antenna shown in Fig. 8, for different tower models.

but may be not satisfactory for supporting towers. It is shown that by omitting supporting towers from the simplified model the input impedance of the antenna is not changed much, i.e. that mutual coupling between the T-antenna itself and supporting towers is relatively small. Hence, we conclude that simplified wire model probably suffices for precise modeling of such antenna. Fig. 13 shows input admittance of the antenna for precise model (shown in Fig. 1) and simplified wire model (shown in Fig. 12). Good agreement between results obtained by these two model is observed.

As a second example let us considered scaled model of anti-fading antenna from ref. [18], the model of which is shown in Fig. 14(a). The antenna is of dipole type. Each arm is in the form of cylindrical mast, whose length is 1100 mm and diameter is 12 mm. The cage, whose length is 550 mm and diameter is 32 mm, is connected to the top of each arm. The generator is connected between the middle of each arm and the nearest end of corresponding cage. A capacitor is placed at the beginning of two-wire line. (On the other side the line extends to two arms of the antenna.) The mast and the cage are modeled in three ways: full plate model (Fig. 14(b)), plate model of the mast and wire model of the cage (Fig. 14(c)), and full wire model (Fig. 14(d)). Note, that in this case the cage can not be modeled by

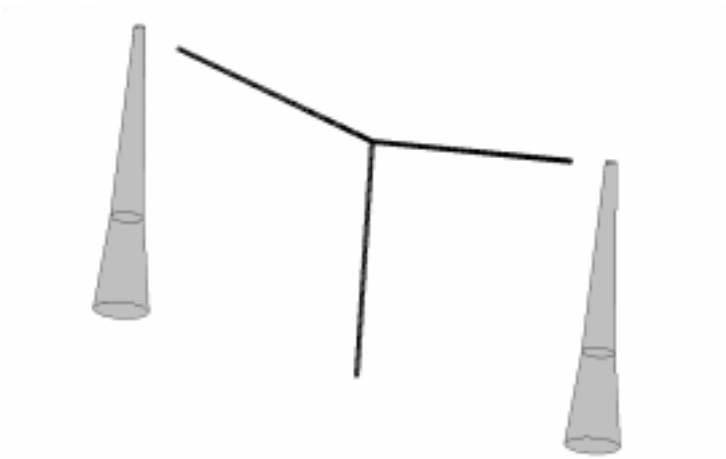


Fig. 12. Simplified wire model of antenna shown in Fig. 1.

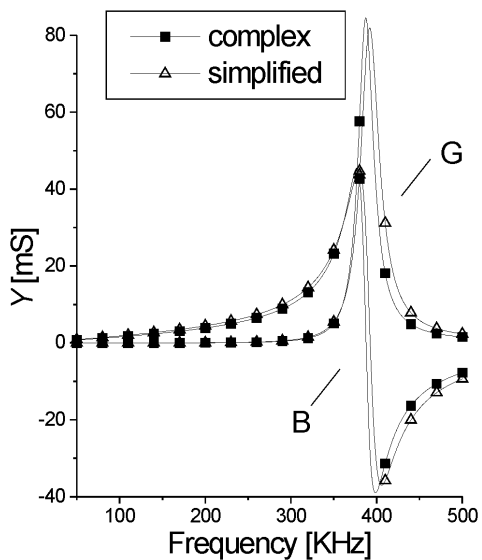


Fig. 13. Input admittance of two equivalent models of T-antenna, shown in Figs. 1 and 12.

single wire. It is shown that all three models give almost the same results. Fig. 15 shows gain of the antenna for different length of two-wire line. The results are in very good agreement with measured results from ref. [18].

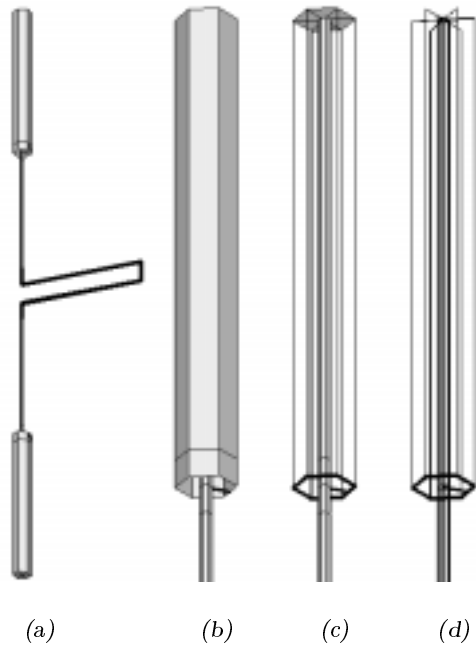


Fig. 14. (a) Full model of anti-fading antenna. Models of one arm: (b) plate, (c) wire-to-plate, and (d) wire.

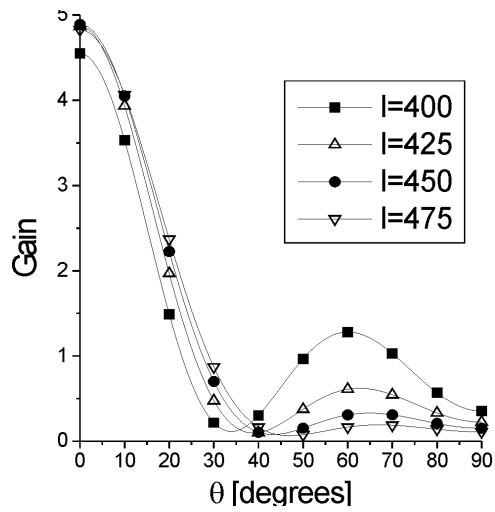


Fig. 15. Gain of anti-fading antenna from Fig. 14, for different lengths of two-wire line.

## 5. Conclusion

Modern numerical methods enable very precise modeling of antenna towers, taking into account all details of their complex mechanical construction. From the electrical point of view this complex construction can be equivalented by single wire in the case of thin towers and those thick towers, whose fulfillment factor is relatively large. The only exception is thin cage towers with the antenna mast inside.

## REFERENCES

1. J. S. BELROSE: *VLF, LF and MF Antennas*. in A. W. Rudge, K. Milne, A. D. Olver, P.Knight (Edts.) *The Handbook of Antenna Design*, vol. 2, London, Peter Peregrinus Ltd., 1983.
2. E. A. LAPORT: *Radio Antenna Engineering*. McGraw-Hill Book Co., 1952.
3. H. E. POCKLINGTON: *Electrical Oscillations in Wires*. Cambridge Phil. Soc. Proc., vol. 9, pp. 324-332, 1897.
4. J. LABUS: *Mathematical Calculation of the Impedance of Antennas*. Hochf. Und Elek, 41, p.17, 1933.
5. E. SIEGEL, J. LABUS: *Scheinwiderstand von Antennen*. Z. Hochfrequenztechn, vol. 43, p. 166, 1934.
6. E. HALLEN: *Theoretical Investigation into the Transmitting and Receiving Qualities of Antennas*. Nova Acta Soc. Sci. Upsal., pp. 1-44, 1938.
7. R. W. P. KING: *The Theory of Linear Antennas*. Cambridge, Mass., U. S. A., Harvard Univ. Press, 1956.
8. R. F. HARRINGTON: *Field Computation by Moment Methods*. New York, Macmillan, 1968.
9. E. K. MILLER, F. J. DEADRICK: *Some Computational Aspects of Thin-Wire Modeling*. in R. Mittra (Ed.) *Numerical and Asymptotic Techniques in Electromagnetics*, Springer, 1975.
10. B. D. POPOVIĆ, M. B. DRAGOVIĆ, A. R. ĐORĐEVIĆ: *Analysis and Synthesis of Wire Antennas*. Chichester - New York, Research Studies Press (John Wiley & Sons), 1982.
11. A. R. ĐORĐEVIĆ, M. B. BAŽDAR, T. K. SARKAR, R.F. HARRINGTON: *Analysis of Wire Antennas and Scatterers*. (Software and User's Manual), Norwood, Artech House, 1995.
12. B. KOLUNDŽIJA, B. RELJIĆ: *Plate Modeling of Wire Structures*. Proc. of IEEE AP-S Int. Symp., Montreal, pp. 1798-1801, 1997.
13. B. M. KOLUNDŽIJA, J. S. OGNJANOVIĆ, T. K. SARKAR: *WIPL-D: Electromagnetic Modeling of Composite Metallic and Dielectric Structures*. (Software and User's manual), Norwood, Artech House, 2000.
14. B. M. KOLUNDŽIJA, B. D. POPOVIĆ: *Entire-domain Galerkin Method for Analysis of Generalized Wire Antennas and Scatterers*. Proc. IEE, Pt. H, vol. 139, pp. 17-24, 1992.
15. B. M. KOLUNDŽIJA, B. D. POPOVIĆ: *General Localized Junction Model in the Analysis of Wire-to-Plate-Junctions*. Proc. IEE, Pt. H, vol. 141, pp. 1-7, 1994.

16. B. M. KOLUNDŽIJA, M. S. TASIĆ, A. R. ĐORĐEVIĆ: *Optimal Wire-Grid Modeling Based on Conversion of Solid Surface Model*. Proc. of IEEE AP-S Int. Symp., Boston, pp. 592-595, 2001.
17. J. SURUTKA: *Uticaj napajanja na vertikalnu karakteristiku zracenja antifeding antena*. Beograd, Publikacije elektrotehnickog fakulteta (serija: Telekomunikacije i elektronika), no. 12, 1959.